

OPTIMISATION OF CT SIMULATION SCANNING PROTOCOLS – ADVANTAGES IN STEREOTACTIC RADIOSURGERY AND STEREOTACTIC BODY RADIATION THERAPY

M.Ș. BÂRHALĂ^{1,2}, T. POPESCU- BÂRHALĂ^{1,2}

¹ *University of Bucharest, Faculty of Physics, Bucharest-Măgurele, Romania*

² *Radiotherapy Department, Neolife, Bd. Ficusului, Bucharest, Romania*

E-mail: mihai.barhala@gmail.com

Abstract. Given the continue desire to increase accuracy and precision in the delivery of radiotherapy treatments, new methods are needed to minimize the uncertainties that can arise throughout the treatment chain. One of the key elements in the accuracy of treatment delivery is the images acquired by CT scanner. Based on this information, the geometric localization of the volume to be irradiated, generically referred to as the target volume, as well as the virtual calculation of dose absorbed inside the patient are performed. With the technological evolution, it is necessary to update the procedures used for patient scanning, given the increased detection and processing capabilities, in order to obtain more qualitative and ultimately more clinically conclusive data. This issue becomes increasingly significant in short session treatments (1-5) fractions. Given the low number of fractions, relative to conventional treatments with around (20–25) fractions, the random element of error starts to become non-mediating and can produce significant deviations in treatment delivery if this aspect is not adequately compensated for. The aim of this work is to test and optimize the CT scanner acquisition and processing parameters so that the data series used to perform the entire chain of processes will ultimately produce a decrease in the uncertainty of treatment delivery. Specifically, the available reconstruction algorithms are tested as well as the modification of slice thickness, slice-to-slice thickness and scan diameter.

Key words: Radiotherapy, radiosurgery, CT simulation, Scanning protocols

1. INTRODUCTION

Given the general approach of modern radiotherapy, the usual workflow for 3D imaging-based treatments has one of the core elements, the computed tomography (CT) simulation. Broadly speaking, the “simulation” is the process in which the anatomy of the patient is converted into a set of data, according to the used imaging modality. Based on those data, in accordance with the clinical information, the radiation oncologist will prescribe the desired dose that will be delivered to the target and will delineate the gross tumor volume (GTV), clinical target volume (CTV) and nearby organs at risk, on the simulation data. The final target volume, namely the planning target volume (PTV), on which the dose is prescribed, will be defined as a margin [1] from the CTV, taking into account specific types of errors. Also, those data are required so that a pre-treatment dose calculation can be performed and estimate with a certain degree of confidence [2], the target volume dose coverage and organs at risk doses, task performed by the medical physicist with the help of the treatment planning system (TPS). Dose calculation algorithms specific to the TPS, require specific measured data [3] in order to perform accurate dose calculations with a high degree of confidence. This is even stricter when the treated targets such as SRS/SBRT lesions are similar in size or close to the size of the radiation source [4].

For radiotherapy purposes, the main modality that allows the dose calculation in the patient is the CT acquisition. In order to perform such task, a link between the attenuation coefficient or Hounsfield Units (HU) for each voxel from the CT dataset and the physical properties, described by relative electron density (RED) or physical density (PD) for each material present in the patient, must be performed [5]. Such link is described by the CT calibration curve, which associates the HU value for specific materials, with very well-known physical properties, inserted in form of rods in a dedicated phantom. Keeping in mind that the attenuation coefficient is dependent on the radiation beam energy, the CT calibration curve is highly influenced by the acceleration voltage of the CT X-ray tube.

Besides the X-ray tube acceleration voltage, a CT scanner has multiple parameters that can be adjusted in order to perform data acquisition such as scanning length, slice thickness, couch pitch and speed, distance between slices, electron current, collimator aperture, beam filter, region of interest (ROI), pixel grid and reconstruction algorithm [5][6]. The variation of those parameters influences the quantity and quality of collected data, thus the accuracy of radiotherapy treatment plan. Regarding the scanning length, this parameter is defined by the cranio-caudal limits indicated by the radiation oncologist for each individual patient, such that the anatomical landmarks and the neighboring organs at risk could be observed completely. If the landmarks are not respected

accordingly, the CT data outside the region is irrelevant thus giving the patient a supplementary dose without any medical significance. In parallel, if the scan is too short, the neighboring organs might not be described completely, thus the calculated dose received by the organs at risk might be incorrect.

The slice thickness is one of the parameters that is directly given by the limitations of the hardware, more specifically by the smallest unit of the detection system. This parameter, in combination with the pitch, couch speed and the collimator aperture influence the delivered dose and define the thickness of each transversal plane of the scan, more specifically, the voxel depth. Generally speaking, it is desired to have the slice thickness as small as possible for high Z-axis (patient length) resolution. The common practice is to use slice thickness of 2.5mm or 1.25mm (if available) for conventional radiotherapy plans, and 1.25mm or smaller (0.625mm for example) for stereotactic plans.

The distance between slices is essentially that between two centers of consecutive slices of a given thickness. This parameter usually has the value equal to the slice thickness but can be modified to higher or smaller values. If the selected value is higher than the slice thickness, then the CT dataset will have fewer data and will have a chance to miss important clinical data, since this variation will create a “data gap” between slices. Opposite if the value is lower than the slice thickness, the sampling on Z-axis will significantly increase up to a factor given by the ratio of those two parameters, thus generating a CT dataset with an apparent slice thickness smaller than the smallest available slice thickness.

The electron current is one of the parameters that significantly increase the homogeneity of pixel HU since the increase of photon flux that passes through the body of the patient will be greater. In this case, the available data for processing will increase. This phenomenon is known as decreasing of quantum noise since the attenuation coefficient is given by the probabilistic interaction of photons with matter. In parallel, the increase of current will also increase the photon fluence and specifically the dose absorbed by the patient.

Regarding the ROI, this parameter defines the diameter over which the data will be reconstructed [7]. Broadly speaking, this parameter is interconnected with the pixel grid since its variation modifies the pixel size for the transversal plane. This variation is caused because the fixed number of available pixels for each transversal plane is allocated to the whole surface defined by the ROI [8]. As a good intuitive example for this behavior, if the ROI is as close as possible to the patient diameter, all the available pixels will take values that will describe the tissues inside the patient and the spatial resolution, and the contrast will be enhanced. Also, the in-plane pixel size will be defined by the ROI divided by the number of pixels that define the body of the patient. Opposite,

if the ROI is significantly larger than the patient's diameter, a considerable number of pixels will describe the structures around the patient, mostly air, thus giving irrelevant clinical information, decreasing contrast and resolution since pixels size will be significantly increased.

One of the parameters that is usually used only for the diagnostic procedures using the CT scanner is the reconstruction algorithm. This parameter modifies the reconstruction kernel that transforms the intensity of the emergent beam, incident on the detector, into 2D planar HU matrixes, according to the rest of the parameters. In essence those kernels are mathematical functions that help in enhancing the CT image quality. Usually for radiotherapy and CT calibration curve, the protocol states a fixed acceleration voltage and one specific reconstruction algorithm that will be used for the dedicated radiotherapy scans.

This paper aims to investigate the influence of variation of the above mentioned parameters and to develop a possible workflow in the clinical practice that could further improve the accuracy in structure contouring and implicit in treatment delivery by means of generating reconstruction CTs.

2. MATERIALS AND METHODS

In the first part of this work, a dedicated CT calibration curve of a phantom was scanned, namely GAMMEX Model 467, with cylindrical rods ranging from lung tissue up to cortical bone, inserted in a solid water phantom, with a GE Discovery RT CT scanner. This phantom was scanned with a radiotherapy protocol, scanning length adjusted to the CT scout images, slice thickness of 0.625mm, as well as distance between slices, 120 kVp acceleration voltage, variable electron current, with a maximum of 400mA, ROI was set to 36cm, as close as possible to the phantom diameter and the "Standard" reconstruction algorithm was used. The number of pixels available for each transversal slice is set to 512×512 .

After the data acquisition, a series of CT reconstructions were generated using the dedicated software, in which the following parameters were modified in the following way: distance between slices was varied with increment of 0.1mm, down to 0.1mm, ROI was varied from the ideal 36cm diameter, up to 80cm, the upper limit of this parameter and all the reconstruction algorithms were applied one by one on independent CTs. The reconstruction algorithms that are available for this CT scanning system are the following: Standard, Soft, Detail, Chest, Lung, Bone, Bone+, Edge. Each reconstruction CT had only one parameter modified so that the differences could be observed relative to the standard acquisition. Beside the reconstructions above

mentioned, a couple of scans with modified electron current were also performed on the phantom in order to establish the influence of this parameter.

The CT scans were exported in the Varian Treatment Planning System (TPS), Eclipse, and a structure set was generated for each individual CT scan. For each individual CT scan, the following structures were generated: BODY, LN-300 Lung, LN-450 Lung, Adipose, Breast, Solid Water 1-4, Real Water, Brain, Liver, Inner Bone, B200 Bone, CB2-30% & 50% Bone and Cortical Bone. All the structures generated beside the BODY, are represented by a cylindrical structure that only encompass the core of each insert, far from the edge of insert to phantom interface and also not including the insert that is left outside of the phantom since the HU of that region is significantly different from the HU on the inserts inside the phantom, due to spectral changes. All those cylindrical structures have the same volume (of about 10 cm³) and are centered on each insert, on each CT, so that the data analysis is relevant and comparable. For each insert, from every CT scan, the mean HU value and the standard deviation were collected and plotted against the relative electron density of each insert.

A sub-analysis of those data was focused on the variation of pixel size and standard deviation with increase of ROI. Also, a set of inserts with different HU values, Cortical Bone, Real Water and LN-300 Lung were analyzed by means of transversal rod diameter with ROI increase.

In the second part of this work, a series of previously scanned patients were used, especially one head, one lung and one bone metastasis, dedicated for stereotactic treatments. Based on those initial scans, the reconstruction CT were generated, by adjusting the scan length and ROI if possible and, at the end, the reconstruction algorithm was modified. This analysis is focused on determining the optimal parametrization for reconstructions, to enhance the contrast and accuracy of target delineation, particularly for small lesions such as for stereotactic treatments. The procedure for this analysis was focused on choosing a specific direction that could encompass different tissues/interfaces.

3. RESULTS AND DISCUSSIONS

The observations regarding the reconstruction algorithms were made relative to the standard acquisition since the CT manufacturer does not provide the mathematical function of each algorithm, thus not having a mathematical description of the behavior of the variations. For this reason, the behavior of each algorithm might be biased by our interpretation of the data. A general observation regarding most of the reconstruction algorithms, namely Lung, Bone, Bone+ and Edge, is that the HU values for each pixel

are increased or decreased depending on the HU value of the neighboring pixels, to be more specific, on the HU value gradient. For this reason, if there is an interface of low-density tissue (low HU value) to water-like density tissue (HU around 0) the HU value for the pixels at the interface will be modified. The strength and the length over which this modification will occur is dependent on the reconstruction algorithm, from our observations, the most “powerful” being the Lung algorithm. Furthermore, a key aspect that is linked to the behavior stated above, is that variations from low density tissue to water-like density tissue is capped at around $\pm(300-400)$ HU because of the lower threshold of possible HU values for low density tissues (-1024 HU). In contrast, at interfaces of water-like density tissue to high density tissue, such as bone or even denser materials as implants, the HU variations significantly surpass the values stated earlier, reaching values up to $\pm(800-900)$ HU. To a certain extent, if the CT value range is defined by 12-bit scale, the upper limit for high density tissue is 3071 HU. If a 16-bit scale is implemented, the upper threshold is significantly increased, giving the possibility of higher variations [9].

The general conclusions that could be drawn from the comparison of the reconstruction algorithms, relative to the Standard algorithm, are the following: i)Soft algorithm decreases the noise in all the tissues by averaging HU values, thus generating more homogenous media but with a lower contrast at interfaces. This leads to a more difficult distinction between tissues with close HU values and a poorer definition of anatomical structures boundaries; ii)Detail algorithm slightly modify the HU values for the pixels, even in high gradient regions, without any significant increase in noise in homogeneous tissues; iii)Chest algorithm is similar to Detail one but the variation of pixel HU value is higher in low density media; iv)Lung, Bone+ and Edge algorithms, in this decreasing order, influence all the tissues whenever there is a HU gradient; v)Bone algorithm produces a significant variation of HU values but only near and inside high density structures.

From the first experimental part of this work, it was noticed that the mean HU value over the defined cylindrical structure of a specific insert, for all reconstruction algorithm has approximatively the same mean HU, up to $\pm(20-30)$ HU for the densest materials available, but the standard deviation has significant variations, depending on the reconstruction algorithm used, up to 4 times the standard deviation for the standard acquisition, compared with the Lung algorithm. This behavior is due to the increased variation of neighboring pixels HU value in the same defined volume, given by the specific processing of this algorithm. These results are presented in Fig. 1.

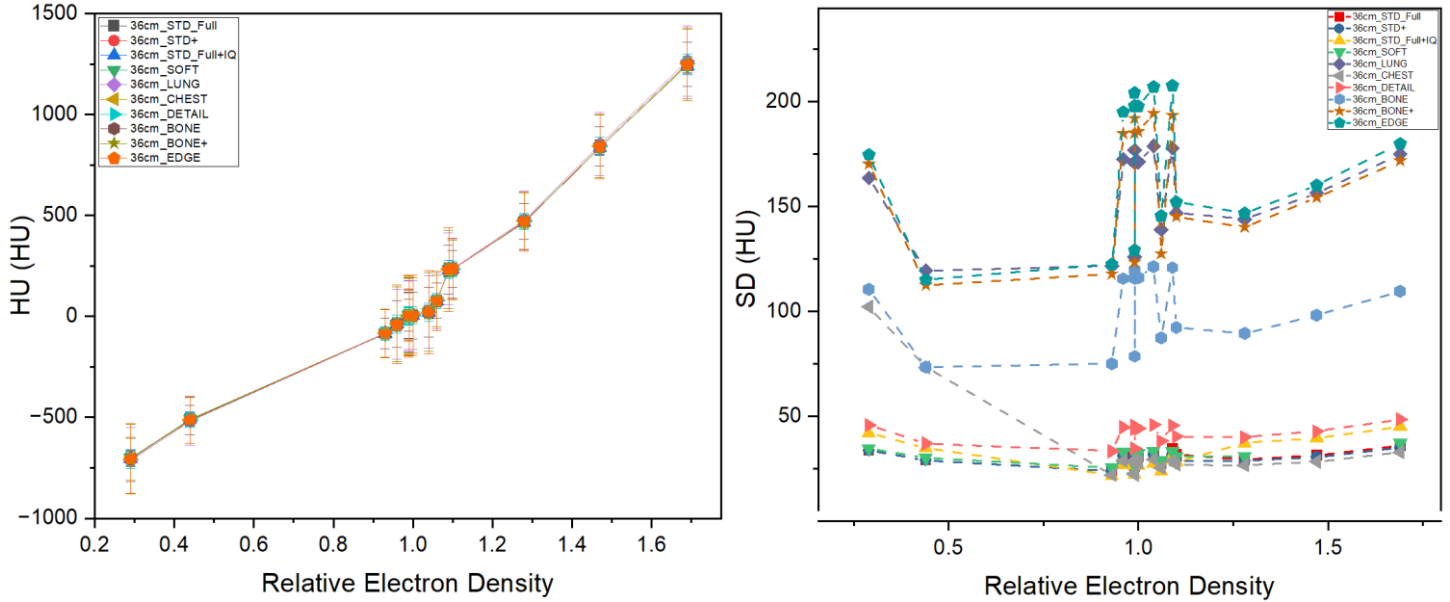


Fig. 1. (Color online) Mean HU (left) and standard deviations (right) over the defined cylindrical volume in the dedicated CT-calibration curve of the phantom

Using the same acquired data but comparing only the Standard reconstruction algorithm against ROI variation, it has been observed that the mean HU of each insert is almost identical for all the ROI dimensions. The distinctive behavior for those scans is that when the ROI is increased, for example at 80cm diameter, the pixel dimensions is increased to $(1.563 \times 1.563) \text{ mm}^2$. This value, as well as for small ROI is calculated directly by dividing the ROI value by the number of available pixels in the transversal plane, on one of matrix axis. For CT scanners with 1024×1024 pixel matrix, the pixel size can be further decreased up to $(0.0977 \times 0.0977) \text{ mm}^2$ for a 10cm diameter ROI. Regarding the standard deviation measured in each cylindrical structure, as the ROI is increased, the standard deviation decreases since the number of voxels composing the volume is lower. The opposite can be observed of the ROI is decreased. This denotes that CT scan acquired with large ROI values tend to be blurrier compared to the ones acquired with adjusted ROI, with a significant loss of contrast, due to the number of pixels describing anatomical features. All those elements are displayed in Fig. 2.

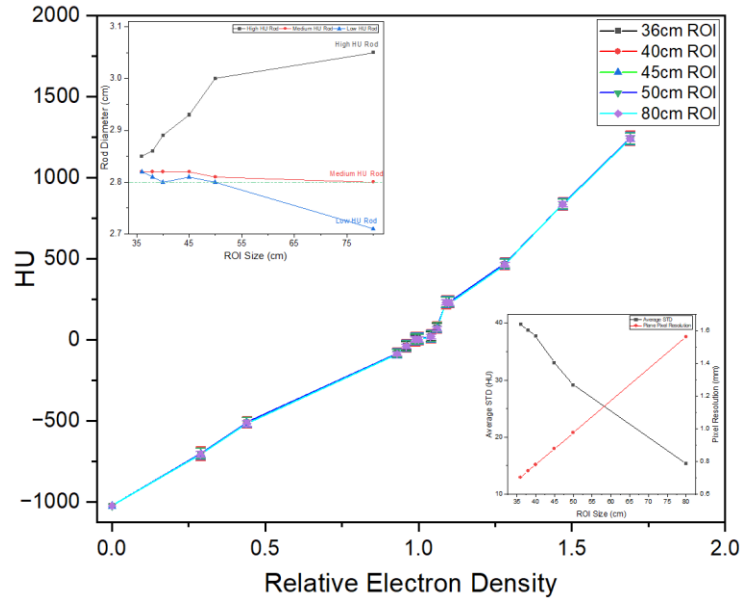


Fig. 2. (Color online) Mean HU variation, pixel size and HU standard deviation behavior with the variation of ROI. In-plane size variation of high, medium, and low HU rods with the variation of ROI

As one can see from the top-left part of the Fig. 2, different rods with variable density have been analyzed by means of in plane diameter, with the variation of the ROI. This analysis was performed by measuring the full width half maximum (FWHM) of each specified insert, at variable ROI, and compared with the true size of the inserts given by the manufacturer. It can be said that for high density structures, the measured FWHM tend to increase, reaching a difference of about (2-3)mm at the maximum ROI. In contrast, for low density structures, the measured FWHM decreases with increasing ROI size, seeming like the structure is shrinking. For the structures with HU value close to 0 HU, the size tends to remain constant throughout all the values of the ROI.

For the analysis of the patient specific CT scans, there were also generated reconstruction CTs with the ROI only focused on the target structure, cropping the rest of the data around that region. By doing this, the spatial resolution of the small ROI CT increased significantly but when the images were compared via Image Registration, in the Eclipse, a diagonally induced shift was observed, increasing with the decrease of ROI of the reconstruction CT. Since the CT scans are related to a specific patient, to a specific series, after importing the small ROI CT, the original CT and the new one are pre-registered and do not allow any new registration to fix this shift. This behavior

should be taken into account and specific reconstruction procedures must be used so that the real matching between CT datasets could be achieved.

For the second part of this work, the three patients were analyzed in the same manner, so the result will be only for the head case since the same behavior was observed for all the cases. For a better understanding of this procedure, the analyzed trajectory and the HU values along the path are displayed in the Fig. 3.

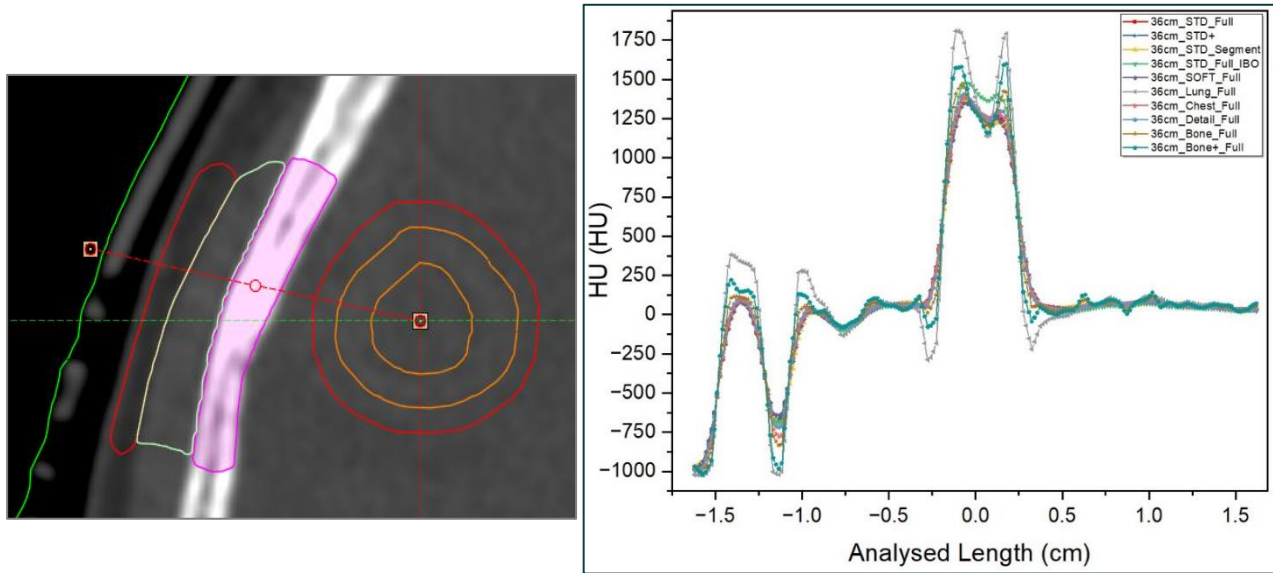


Fig. 3. (Color online) Analyzed trajectory for the stereotactic head case and the HU values along the path for different reconstruction algorithms

The analyzed path for this particular case was air – SRS mask – air – skin – adipose tissue – muscle – dense bone – brain. As stated before, the algorithms that produce the greatest HU variation is Lung, as it can be seen from the material junctions. The most significant variation appears when passing from air to SRS mask (~ -1000 HU to 0 HU) or from muscle to dense bone (~ 0 HU to 1600 HU). Due to the characteristic effect of some reconstruction algorithm, it can be seen both from Figs. 3 and 4 that in homogenous media, such as brain tissue, a noise starts to appear. Due to the significant variation of HU, an increased contrast is created at those junctions, as it can be seen from Fig. 4, leading to sharper edges. In order to have a consistent evaluation the HU window was kept identical for both CTs.

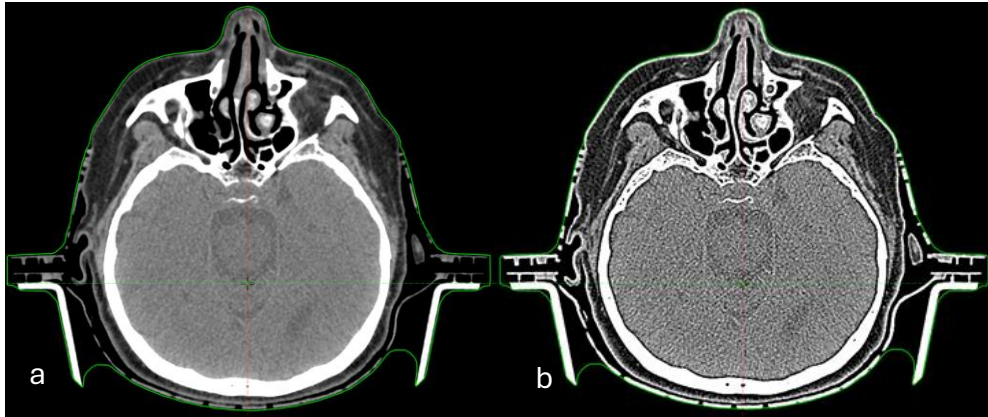


Fig. 4. (Color online) Visual difference between CT acquisition with Standard algorithm (a) and with Lung algorithm (b)

When analyzing the absolute variation of the HU values, as compared with the Standard reconstruction algorithm, we can see variations of around 600 HU, at muscle – dense bone interface, while using the Lung algorithm. The same behavior was observed for all three patients but to a lesser extent since there were not any tissue junctions with such great HU variation as in the head case. The result of this analysis can be observed in the Fig. 5. An interesting behavior observed during the data analysis is that the sub-algorithm Standard – IBO increased the HU in the high-density structures and decreases slightly the HU of water-like density structures. This behavior has been observed both in Fig. 3 and Fig. 5 but requires further investigation to accurately describe the variation pattern.

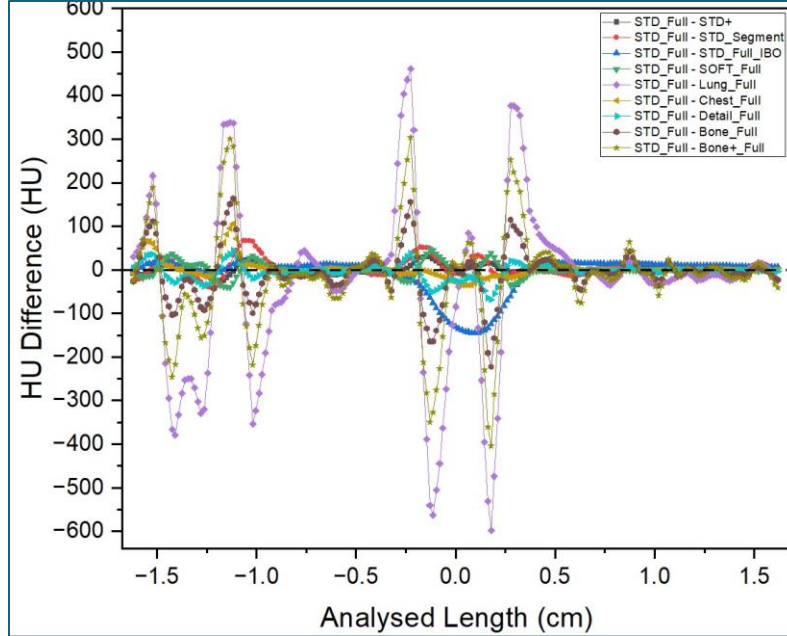


Fig. 5. (Color online) HU difference between the Standard reconstruction algorithm and the rest of available reconstruction algorithms along the analyzed path

4. CONCLUSIONS

For each CT scan, using a conventional protocol, without regarding the reconstruction algorithm, acceleration voltage and electron current, that parameters that can easily improve the quality of the scan are the scanning length, slice thickness and ROI. The adjustment of those three parameters can significantly improve the spatial resolution on all axes, with little to no effort, thus increasing the accuracy of anatomical structure recognition and delineation. Even though this idea can be as well applied to scans for conventional radiotherapy, we should minimize all possible errors and uncertainties.

In order to enhance accuracy of structure definition, the usage of an additional CT scan, namely a reconstruction CT scan, is recommended. It has been shown that reconstruction algorithms such as Lung, Bone+ and Bone provide significant increase in contrast, especially at high HU gradients. This might offer significant advantages when the target is very close to a high gradient region, such as bone or lung.

Beside the variation of the reconstruction algorithm itself, an additional CT reconstruction with small ROI only focused on the lesion region, with the thinnest slice thickness available and with the smallest distance between slices, represents a viable alternative. An aspect that should be taken care of is the induced shift that appears after importing the reconstructed CT.

As a general workflow, one can mainly adjust the parameters in order to be specific to each patient. If further details are desired, the first and the second reconstruction can be generated after the initial scan was performed, without any supplementary irradiation of the patient. Once the desired scans are imported, a workflow similar to 4DCT target delineation is approached, to be more specific, the structures are delineated on the reconstructed CT and copied to the standard CT. After this step has been completed, the usual 3D-based radiotherapy can be performed on the standard CT scan.

Since this analysis was performed on a specific CT scanner, one should investigate its own CT scanner parametrization and also, the available variables in order to achieve the desired results and to apply the workflow.

Acknowledgments. The authors thank Neolife Bucharest for having the opportunity to perform the measurements in the Radiotherapy Department.

REFERENCES

1. M. Van Herk, *Errors and margins in radiotherapy*, Semin. Radiat. Oncol., **14**(1),52-64, (2004).
2. D. van der Merwe, J. Van Dyk, B. Healy et al., *Accuracy requirements and uncertainties in radiotherapy: a report of the International Atomic Energy Agency*. Acta Oncol., **56**(1), 1-6, (2017).
3. M.S. Barhala, T. Popescu, *The influence of LINAC and beam scanning system mechanical components in relative dose measurements*, Rom. J. Phys., **70**, 702 (2025).
4. T. Popescu, M.S. Barhala, *Variability of detector-to-detector response in small field relative dosimetry*, Rom. J. Phys., **70**, 704 (2025).
5. W. Schneider, T. Bortfeld, W. Schlegel, *Correlation between CT numbers and tissue parameters needed for Monte Carlo simulations of clinical dose distributions*, Phys. Med. Biol., **45**(2), 459-478, (2000).
6. A. T. Davis, S. Muscat, A. L. Palmer., D. Buckle, J. Earley, M. G. J. William, & A. Nisbet, *Radiation dosimetry changes in radiotherapy treatment plans for adult patients arising from the selection of the CT image reconstruction kernel*, BJR open, **1**(1), 20190023 (2019).
7. S.P. Raman, M. Mahesh, R.V. Blasko, E. K. Fishman, *CT scan parameters and radiation dose: practical advice for radiologists*, J. Am. Coll. Radiol., **10**(11), 840-846, (2013).
8. R. Chityala , K. R. Hoffmann, D. R. Bednarek, & S. Rudin, *Region of Interest (ROI) Computed Tomography*, Proceedings of SPIE-the International Society for Optical Engineering, **5368**(2), 534–541, (2004).
9. A. Hata, M. Yanagawa, O. Honda et al. *Effect of Matrix Size on the Image Quality of Ultra-high-resolution CT of the Lung: Comparison of 512×512 , 1024×1024 , and 2048×2048* , Acad. Radiol., **25**(7), 869-876, (2018).